Liu *et al. Journal of Orthopaedic Surgery and Research* (2025) 20:319
https://doi.org/10.1186/s13018-025-05681-8

Journal of Orthopaedic Surgery and Research

RESEARCH **Open Access**

A novel external fixation for treating tibial fractures: a finite element and biomechanical study

Shen Liu[1], Xiangdang Liang[2*], Songyang Liu[1], Zhanshe Guo[3], Xing Wei[1] and Yonghui Liang[4*]

Abstract

Objective Design a new type of external fixation device that is small in size, high in strength, and capable of achieving the mechanical requirements for fracture healing. Verify the rationality and effectiveness of the device in treating tibial fractures through finite element analysis and biomechanical comparative tests.

Methods Finite element simulation was performed on the new external fixation device to treat fractures, to verify whether the mechanical properties of the device meet the requirements of fracture healing. A fracture gap model was created using Sawbones to simulate midshaft tibial comminuted fractures. The experiment was divided into four groups, testing the mechanical characteristics of the new external fixation (NEF), locking compression plate (LCP), the unilateral external fixation (UEF), and the externalized locking compression plate (E-LCP). The axial compression, torsion, fatigue and ultimate load tests were performed separately. Data were collected and statistical analysis was performed to verify whether there were statistical differences between the four groups.

Results The finite element analysis of NEF demonstrated that the fracture end was displaced by 0.512 mm under 700 N loading, and the maximum stress value of the device was 189 MPa, which met the mechanical requirements. Axial compression tests showed that LCP (2108.596 N/mm) had the highest stiffness, and NEF (519.489 N/mm) had higher stiffness than both UEF (327.153 N/mm) and E-LCP (316.763 N/mm) ($p < 0.05$), but no significant difference between UEF and E-LCP ($p = 0.313$). There was a significant difference in mean torsional stiffness among UEF (1.412 N·m/deg), NEF (1.398 N·m/deg), LCP (1.128 N·m/deg), and E-LCP (0.838 N·m/deg). No structural failures occurred during fatigue testing spanning 108,000 cycles. In ultimate load tests, NEF withstood the highest load, followed sequentially by LCP, UEF, and E-LCP. Significant differences were found between the groups ($p < 0.05$), with frame bending and secondary bone fractures noted in post-test evaluations.

Conclusions The NEF for tibial fractures is well-designed to meet the fracture healing requirements. It has certain advantages in comparison with other fixation methods and can be used as a new method for the treatment of tibial fractures.

Keywords Tibial fracture, External fixation device, Finite element analysis, Biomechanical testing

*Correspondence:
Xiangdang Liang
lxd301@263.net
Yonghui Liang
13910199041@163.com
[1]Department of Orthopaedics, Aerospace Center Hospital, Beijing, China
[2]Department of Orthopedics, General Hospital of People's Liberation Army, Beijing, China
[3]School of Instrumentation Science and Opto-electronics Engineering, Beihang University, Beijing, China
[4]Department of Emergency, Aerospace Center Hospital, 15 Yuquan Road, Haidian District, Beijing 100049, China

Introduction

Although the optimal management of open fractures and severely damaged fractures of the tibia remains controversial, external fixation devices are widely employed for both temporary and definitive treatments owing to their ability to stabilize fractures while preserving soft tissue integrity [1]. Nevertheless, traditional external fixators have significant limitations, including their bulkiness, inadequate stability, and high risk of pin tract infections or delayed union, which restrict their widespread use [2]. Using internal fixation plates as external fixators offers advantages such as compact size, lightweight design, and ease of application, and has been applied in clinical practice [3–6]. However, it has not been further promoted because of its decreased overall mechanical stability by increasing the distance between the plate and the bone [7]. And the design of the locking hole also cannot guarantee its stability.

The role of controlled interfragmentary motion at the fracture site in fracture healing has been a long-standing research focus. Kenwright et al. [8] demonstrated that the mechanical environment significantly influences the healing process. Specifically, controlled stress can enhance the metabolism of bone cells and osteoblasts, thereby promoting bone regeneration. Current evidence suggests that micromotion induced by low-frequency axial stress positively impacts fracture healing. An axial relative micromotion within 0.2–1 mm promotes callus formation, while displacements exceeding 2 mm may disrupt callus formation, leading to nonunion or delayed union [9, 10]. Additionally, shear forces should be avoided as they can generate lateral friction, impeding development and callus formation at the fracture site [11, 12].

In this study, we developed a novel type of external fixation device (NEF) and systematically evaluated the rationality and effectiveness of the device through finite element analysis and a series of mechanical tests in the treatment of tibial fractures.

Materials and methods

Design and fabrication of NEF

The structure of NEF (Fig. 1) consists of a rectangular frame and screws made of titanium alloy material (modulus of elasticity of 105 GPa). The length and width of the rectangular frame are similar to that of the locking compression plate, but the thickness, screw diameter and thread depth are significantly increased, thus increasing the overall strength and stability of the device.

Fully threaded nail holes are present inside the frame, which are locked when the screws are inserted. The raised portion at the bottom of each nail hole increases the

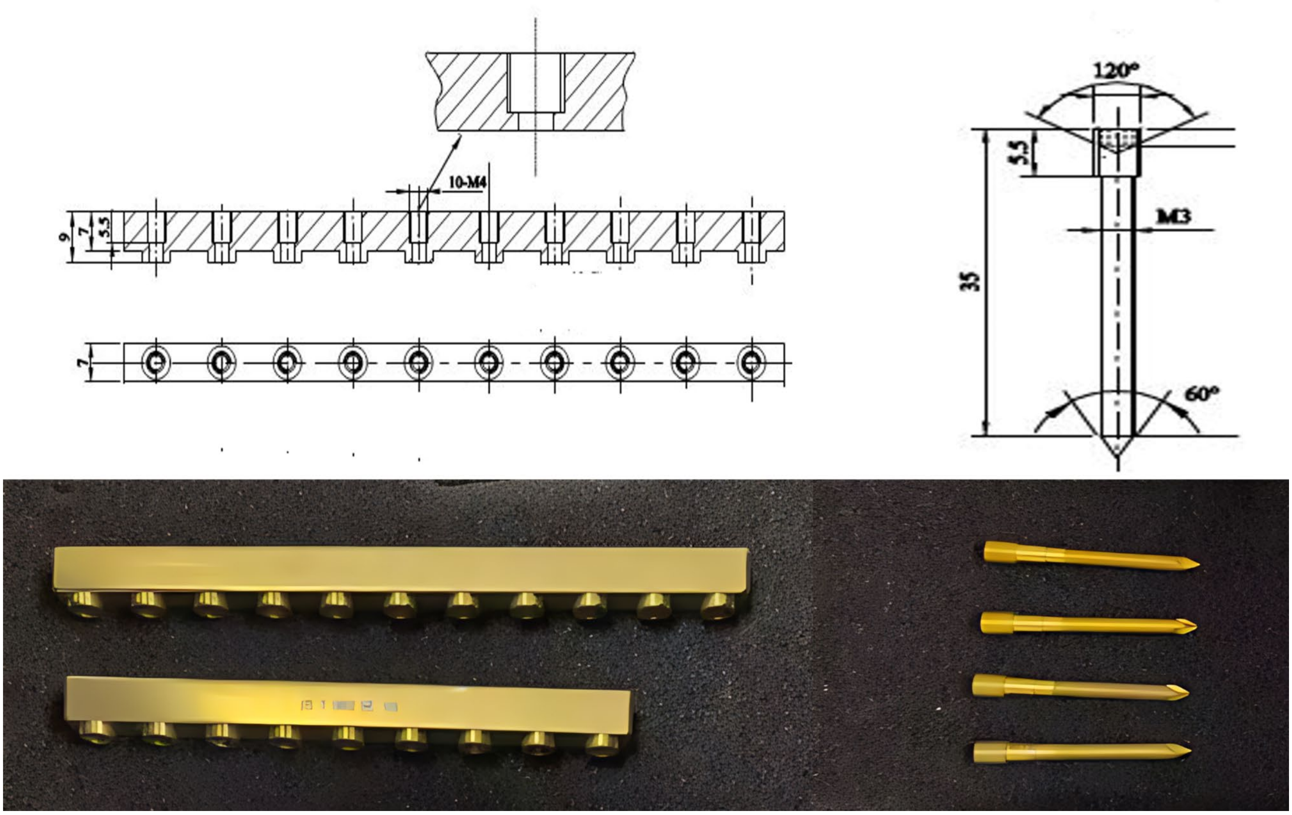

Fig. 1 Planar design and physical diagram of NEF

plate-screw interface, distributes the stress, and enhances angular stability after the screws are tightened. Additionally, this raised portion serves a guiding function.

Furthermore, the raised portion separates the skin from the frame, preventing skin necrosis under prolonged pressure, and facilitating wound observation and postoperative care.

Finite element static analysis

To verify the design rationality of NEF, finite element software (ANSYS Workbench 12.0, ANSYS Inc., Canonsburg, PA, USA) was used for simulation. The model shown in Fig. 2A was established in ANSYS, and the size was strictly in accordance with the actual parameters. The size of the new external fixator body is 12 mm×12 mm×250 mm, the diameter of the screw is 5 mm, and the actual number of screw holes is 6. The mechanical parameters of NEF and screws are input according to the titanium alloy material, with an elastic modulus of 105 GPa and a Poisson's ratio of 0.32. The bone model is a simplified hollow annular cylinder with an outer diameter of 35 mm, an inner diameter of 15 mm, an elastic modulus of 20 GPa, and a Poisson's ratio of 0.25. The distance between the bone and the frame is 20 mm.

All components of the model use Solid95 unit type and are bonded together as a single unit. To improve the accuracy of the calculations, the meshing process divides the key lines at equal intervals: the long side of the fixed frame model is divided into 50 equal parts, and the axis of the bone model is divided into 20 equal parts (Fig. 2B).

The finite element analysis type was set to static. The left end face of the bone model was constrained with 0 degrees of freedom, and a uniform force of 700 N was applied to the right end face. This value was selected to simulate the approximate body weight load during single-leg stance for an average adult (70 kg) [9, 13]. The maximum displacement of the two tibial fracture ends was measured, and the stress distribution of each part of the new external fixator under axial pressure was determined.

Mechanical experiment

Specimen preparation

Fourth generation, large-sized left composite tibia (Sawbones #3401, Pacific Research Laboratories, Inc., Vashon, WA, USA) was used for the biomechanical testing. A fracture gap model was created to simulate comminuted mid-shaft tibial fractures using synthetic composite bones. The bone model was cut in half with a saw to create a 20 mm osteotomy gap.

To examine the mechanical properties of different fracture fixation techniques, twenty tibiae were divided into four groups, with fixation using either NEF, E-LCP, LCP or UEF (Fig. 3). Based on preliminary studies, five specimens from each group were selected.

The detailed procedures for each group were as follows: The fixation devices of four groups were placed on the

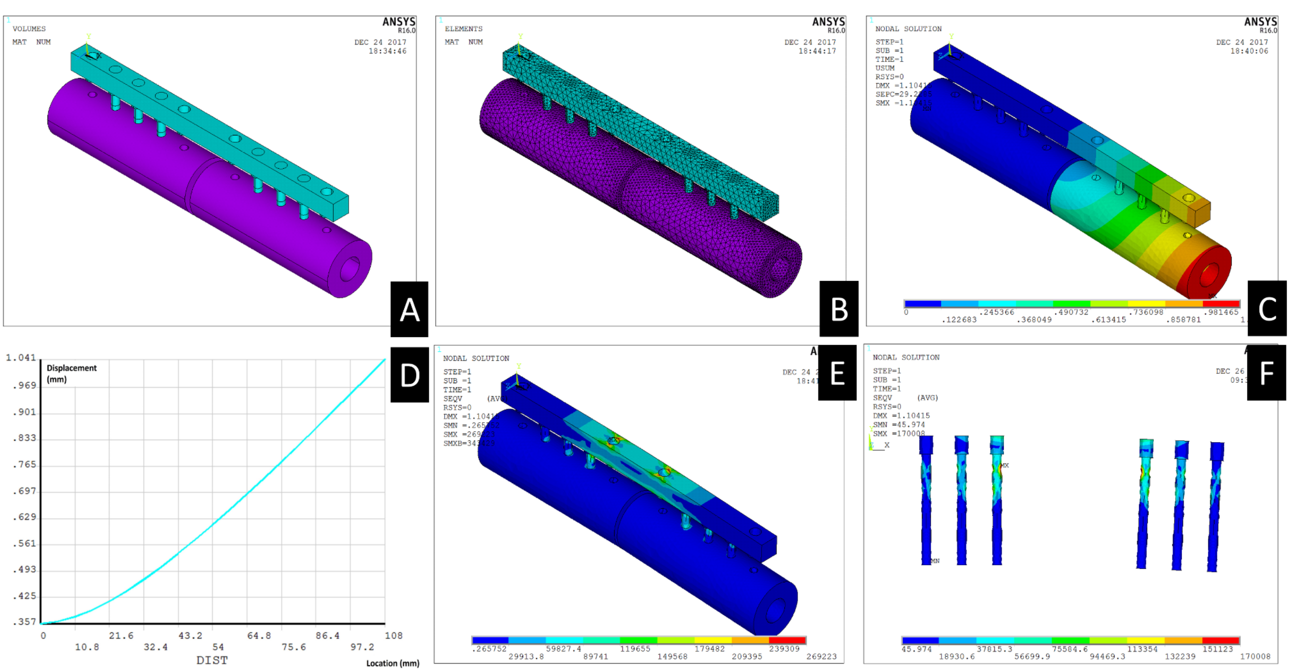

Fig. 2 Finite element analysis. **A**: 3D structural model of NEF in ANSYS. **B**: Meshing result of the finite element model. **C**: Displacement distribution diagram under external force load of 700 N. **D**: The outer diameter axis displacement distribution curve of the right bone model. **E**: Stress distribution diagram of model. **F**: Stress distribution diagram of screw

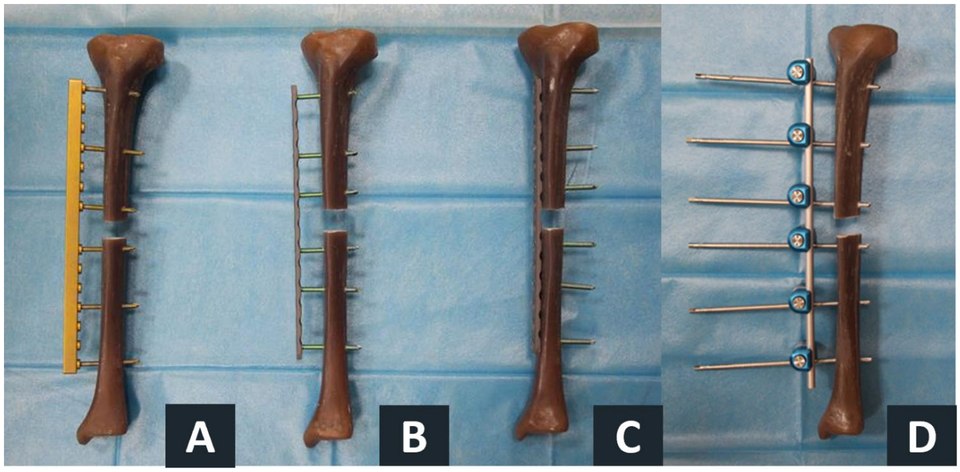

Fig. 3 Four groups of sample pictures (**A**: NEF; **B**: E-LCP; **C**: LCP; **D**: UEF)

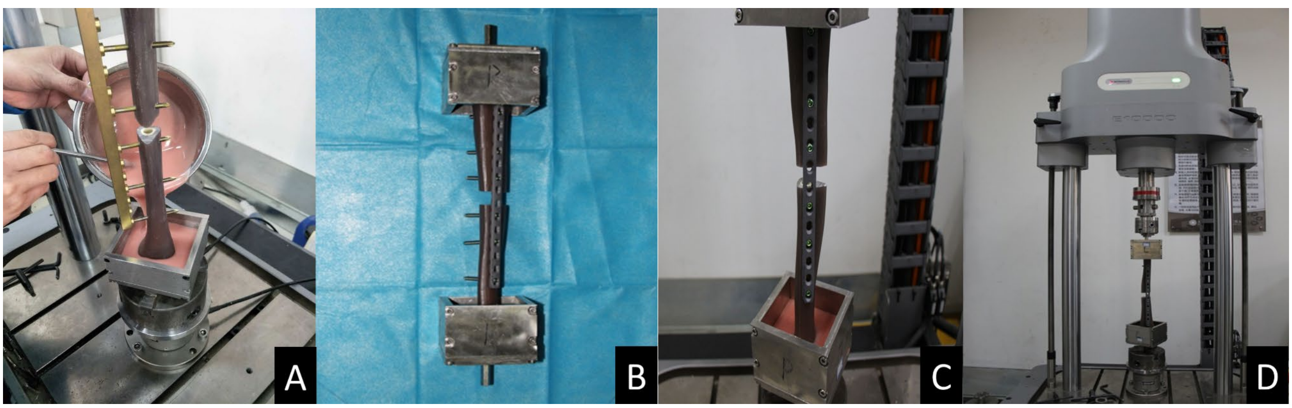

Fig. 4 Sample preparation process for mechanical experiments. **A**: Evenly mix the self-curing dental tray powder and dental water in a mixing ratio of 3:1 (volume ratio), then slowly pour it into the fixture. **B**: After it is completely solidified, embed the other end in the same way. **C** and **D**: The sample is placed on an electronic universal material testing machine and fixed to perform parameter calibration

anterior medial surface of the tibia to stabilize the fractures. In the NEF, E-LCP and UEF groups, the plates/external fixator rods were positioned with 20 mm plate-to-bone clearance. Considering the presence of soft tissues in the clinical reality, this is a more appropriate distance to ensure that the soft tissues of the lower limbs are not compressed by the external fixation device and complications such as skin necrosis occur [5, 14, 15]. In the LCP and E-LCP groups, each tibia was plated on the medial aspect with a 252 mm length, 14-hole titanium broad 4.5/5 mm LCP (Zhengtian, China). Titanium locking screws (5 mm diameter) were inserted into the second, fourth, and seventh locking holes from the middle of the LCP, on both sides of the fracture.

Each screw was tightened to a torque of 10 Nm, as measured with a digital torque meter. In the other groups, screws were inserted sequentially into the same positions with identical torque values. In accordance with tibial fracture surgery principles, all screws or pins were inserted to penetrate both cortices of the Sawbone. All procedures were performed by an orthopedic surgeon and an assistant, following standard protocols.

The proximal and distal ends of tibia were mounted in a custom-made jig, ensuring that the tibia's position aligned with its mechanical axis when the human body moves under load (Fig. 4).

Axial compression testing

The fixed specimens were placed on an Instron E1000 universal material testing machine (Instron, Norwood, Massachusetts) (Fig. 4C and D), and the displacement zero point was calibrated before loading commenced. The tibial axis was subjected to compression from 0 to 700 N at a loading rate of 20 N/s. All operations were performed on the same testing machine at standard room temperature.

Torsion testing

For torsion testing, the maximum torsional load was set to 5 N·m, and the twist angle was initially calibrated to

0°. The torsional moment was based on peak rotational forces during gait cycles, derived from in vivo kinematic studies [11, 15]. Loading was applied at a torsional rate of 0.5 N·m/s. The torsional angle data for each group were then collected through computer instructions.

Fatigue and ultimate load testing

According to the method of axial compression test, a certain number of fatigue tests were conducted on all specimens. The load range was set from 0 to 700 N. Based on the estimated activity of patients with tibial fractures 6 months post-operation (lifting the affected limb for single-leg weight bearing, 1 time, 3 s per repetition, 30 min per day), a total of 108,000 cycles were applied, with cyclic vertical compression at a rate of 70 N/s [13]. The experiment was terminated if the fixture failed, or when the number of compressions was completed. If the fixture did not fail, each specimen in the four groups underwent a single compression test with a load starting at 0 N, at a rate of 20 N/s, until the tibial fracture fixation model failed. The maximum compressive strength and the maximum compressive displacement at failure were then recorded.

Preliminary fatigue tests were conducted on two specimens (one NEF and one UEF) to validate the 108,000-cycle protocol. No early failures were observed, confirming the suitability of the loading parameters.

Statistical analysis

A total of six data points were collected for each specimen in axial compression testing and torsion testing. To account for the creep effect of the sample, the first two data points were discarded, and the remaining four data points were used for final analysis. Each mechanical test was performed three times, and the average value was calculated for data analysis. Statistical analysis was conducted using a one-way ANOVA with Tukey's post-hoc test, with a significance level set at $p < 0.05$. Data are presented as mean ± standard deviation (SD), with SDs calculated individually for each experimental group to reflect within-group variability.

Results

(1) Fig. 2C is a distribution diagram of the total displacement after finite element static analysis. The different colors represent the displacement gradient. Under the applied external force, the displacement of the left half of the bone is minimal (0.003 mm) and falls within the lowest gradient range. In contrast, the displacement distribution on the right half gradually increases from left to right, with the largest displacement observed at the right end face (0.512 mm). Path mapping along the outer surface axis of the right bone model allows the displacement distribution trend of the right bone along the axial direction (X direction) to be visualized in the curve shown in Fig. 2D.

The stress distribution from the finite element simulation analysis is presented in Fig. 2E. The colors represent the stress distribution gradient, with blue indicating lower stresses and red indicating higher stresses. Due to the low elastic modulus of the bone model material, which is much smaller than that of titanium alloy, the fixator and screw structures experience larger stresses. As shown in the figure, the fixator undergoes bending to a certain extent, with the middle portion acting as the primary load-bearing region. The maximum stress occurs at the upper edge of the unused screw hole. Upon analyzing the screws individually, it is evident that screws closer to the inner side bear greater stress (Fig. 2F). The maximum stress value is 189 MPa, which is below the allowable stress for the device material (344 MPa).

(2) The relationship between the load and displacement for each sample is shown in four sets of load-displacement curves (Fig. 5A). The figure demonstrates that the magnitude of the load is linearly related to the displacement, with the slope representing the stiffness value ($K = F / \triangle l$, F: axial force, $\triangle l$: deformation). Under a load of 700 N, the UEF exhibited the greatest displacement, followed by the E-LCP, while the LCP showed the least displacement. The NEF exhibited displacement values between those of the E-LCP and LCP. The compressive stiffness values for the four sets of data from each group were calculated, and the results are shown in Fig. 5B: LCP (2108.596, SD 31.177 N/mm) > NEF (519.489, SD 1.032 N/mm) > UEF (327.153, SD 3.690 N/mm) > E-LCP (316.763, SD 2.556 N/mm). One-way ANOVA was performed on the compression data for the four groups, and the results indicated that $p < 0.05$, suggesting a significant difference between the groups. A Tukey post-hoc test revealed that the compressive stiffness of the NEF was significantly higher than that of both UEF and E-LCP ($p < 0.05$). However, no statistically significant differences were found between EF and E-LCP ($p = 0.313$).

(3) The relationship between torque and angle for each sample is shown in the torque-angle curves of the four groups (Fig. 5C). The figure illustrates that the torque magnitude is linearly correlated with the angle, with the slope representing the torsional stiffness value ($K' = M/\theta$, M: torque, θ: angle). Under the same applied torque of 5 Nm, the torsion angle generated by the E-LCP was the largest, followed by the LCP. The NEF and EF exhibited relatively similar results, with the NEF producing a larger angle than the EF. The torsional stiffness values of the four times data of each group were calculated, and the results are shown in Fig. 5D: UEF (1.412, SD 0.059 N·m/deg) > NEF (1.398, SD 0.001N·m/deg) > LCP (1.128, SD 0.044 N·m/deg) > E-LCP (0.838, SD 0.002N·m/deg). Pairwise comparison results showed that there were

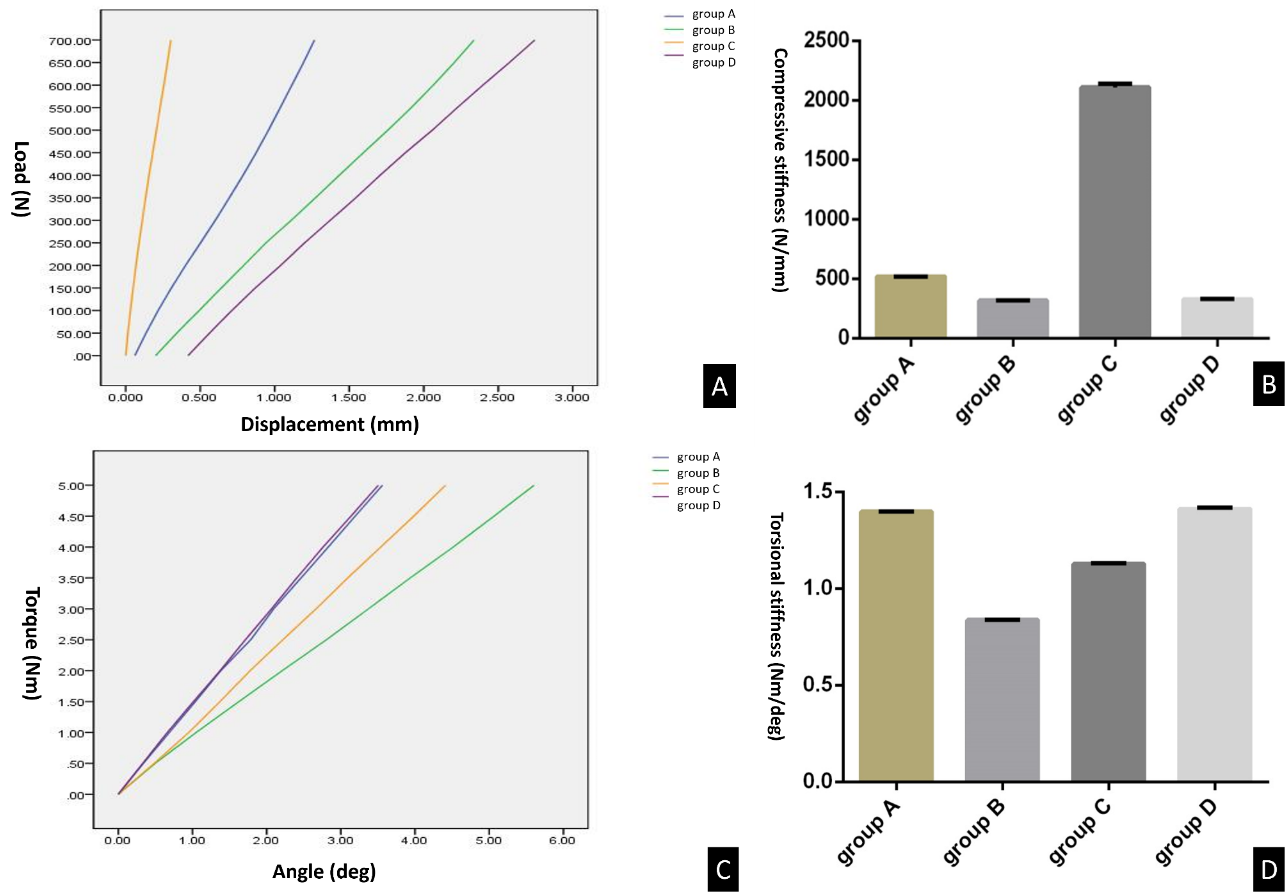

Fig. 5 Biomechanical experimental results of four groups. **A**: Load-displacement curves. **B**: Histogram of compression stiffness. **C**: Torque-angle curves. **D**: Histogram of torsional stiffness

significant differences among the four groups by a Tukey post hoc test ($p < 0.05$).

(4) The four groups of experimental samples underwent 108,000 cycles of compression fatigue testing, during which no failure phenomena—such as model fracture, screw loosening, or frame deformation—were observed. In the ultimate load tests, NEF supported the highest load (5307.374 N), followed by LCP (4030.158 N), UEF (1815.783 N), and E-LCP (1564.900 N). One-way ANOVA revealed a significant main effect among the groups ($p < 0.001$). Post-hoc Tukey HSD tests demonstrated statistically significant differences between NEF and all other groups (NEF vs. LCP: $p = 0.012$; NEF vs. UEF: $p < 0.001$; NEF vs. E-LCP: $p < 0.001$), as well as between LCP and both UEF ($p = 0.003$) and E-LCP ($p = 0.002$). No significant difference was observed between UEF and E-LCP ($p = 0.456$).

Following the ultimate load test, all groups exhibited varying degrees of failure (Fig. 6B), including frame bending, bone model fracture, and screw bending. Frame bending typically occurred at the midpoint of the frame, often accompanied by bending of some screws, which was consistent with the results from the finite element analysis. Bone model fractures occurred at the screw perforation at the lowest end of the tibia (Fig. 6C), presenting as transverse or oblique fracture lines along the direction of the screw hole.

Discussion

Tibial fractures are among the most common long bone injuries. Due to the unique anatomical position of the tibia, it is frequently exposed to high-energy trauma, leading not only to severe fractures but also to significant soft tissue and vascular damage [16]. Traditional treatments, including the use of locking compression plates (LCP) and external fixators (EF), remain standard. In recent years, externalized locking compression plates (E-LCP) have emerged as a promising alternative, garnering significant research interest. Marti and Besselaar [3] first introduced AO plates as external fixators in 1984, demonstrating their efficacy in the treatment of forearm and tibial fractures. Subsequently, Zhou et al. [17] reported a 95.65% fracture union rate in 23 patients with closed distal tibial fractures treated with LCP as an external fixator. Similarly, Luthfi Hidayat et al. [18] observed satisfactory fracture and wound healing outcomes in five

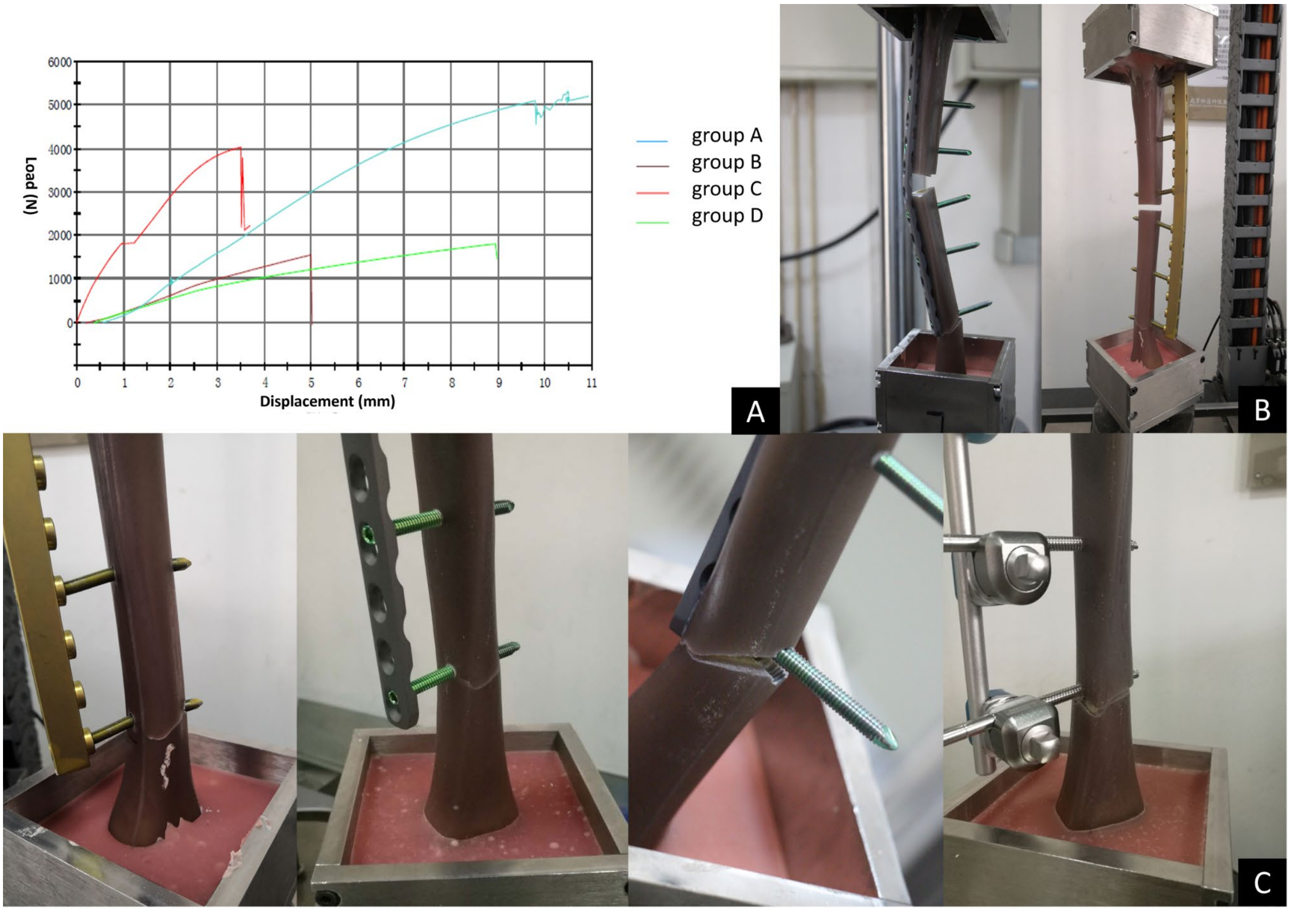

Fig. 6 Ultimate load test results of four groups. **A**: Load-displacement curve of ultimate load test. **B**: The frames of all groups were bent. **C**: Sawbones in all four groups of models were fractured

patients with Gustilo grade III tibial fractures treated with E-LCP. Additional studies [4, 19] have highlighted the advantages of E-LCP in a two-stage protocol for managing open or high-energy tibial fractures. These applications demonstrate that E-LCP offers benefits including minimized tissue trauma, ease of application, minimal impact on the local blood supply to the fracture, and reliable clinical outcomes [20–23]. Furthermore, cost analyses suggest that the E-LCP technique is economically feasible and cost-effective, optimizing healthcare resources for the treatment of open tibial fractures [24]. Despite these advantages, the mechanical stability of E-LCP has been a subject of criticism, as it often fails to meet the necessary requirements for effective fracture fixation, which has limited its widespread clinical adoption. Ahmad et al. [7] explored the relationship between the distance of the LCP from the bone and its stability, revealing that distances under 2 mm maintained structural stability, while distances exceeding 5 mm led to a 63% reduction in axial compressive strength, significantly compromising mechanical integrity. A finite element analysis also indicated that an increased distance from the plate to the bone can result in excessive flexibility, hindering optimal bone healing [25]. To address these concerns, the use of femoral LCPs as a more robust alternative for tibial fracture fixation has been suggested [5, 26].

The novel external fixation (NEF) device builds on the advantages of LCP while addressing its limitations. By increasing the thickness of the frame and deepening the thread locking mechanism, the NEF significantly enhances strength and stability, making it particularly suitable for the management of tibial fractures. Compared to traditional universal external fixators (UEF), the NEF is lighter, more compact, and allows patients to wear normal clothing post-surgery. This design feature facilitates daily activities and rehabilitation exercises after fracture fixation, promoting improved patient mobility and quality of life.

In both finite element analysis and mechanical experiments, simulating comminuted midshaft tibial fractures and choosing appropriate plate-bone distance were essential [27]. Based on previous studies [7, 13, 28], a tibia model with a 1 mm midshaft osteotomy was used to represent a stable fracture, while a model with more than a 5-mm osteotomy was considered an unstable fracture. Ang et al. [15] utilized a 20 mm gap to simulate a comminuted fracture in their study. Following these references and considering practical clinical scenarios, we adopted a 20-mm distance between the two fracture ends in our model. Furthermore, the plate-bone distance for three experimental groups was set to 20 mm to ensure sufficient fixation stability while preventing complications, such as soft tissue compression or skin necrosis, which may occur due to the external fixator [5, 29].

After completing the production of NEF, finite element software was utilized to model its application in the treatment of tibial fractures. Under an axial load of 700 N, which approximates the weight of an average adult, the maximum displacement of the NEF was 0.512 mm. This value aligns with the optimal mechanical environment for fracture healing, which is typically between 0.2 and 1 mm of axial displacement [8, 9]. Additionally, the NEF exhibited a maximum stress value of 189 MPa, well below the material's yield strength limit of 344 MPa. These results indicate that the titanium alloy NEF provides a stable and safe mechanical environment for fracture healing under full weight-bearing conditions, thus supporting the theoretical feasibility and rationality of its design.

When subjected to the same axial load of 700 N, the displacement values of UEF (2.327 mm) and E-LCP (2.138 mm) exceeded 2 mm. This indicates that the fixation methods in these two groups were unable to provide the optimal mechanical environment required for fracture healing under full weight-bearing conditions in adults. In contrast, the displacement value of LCP was 0.256 mm, which aligns with the AO principle of "rigid internal fixation." The NEF, with a displacement of 1.206 mm, fell between the LCP and the two external fixations (UEF and E-LCP), meeting the mechanical requirements for fracture healing. Furthermore, under partial weight-bearing conditions or with the addition of extra screws, it is reasonable to expect the NEF to exhibit even more favorable displacement values for promoting fracture healing.

Shear and rotational loads are known to generate shear forces, which can induce dynamic friction at the fracture ends, leading to lateral dislocation of the fracture and negatively impacting capillary and callus formation at the fracture site [9, 10, 12]. In the torsion experiment, the UEF exhibited the highest torsional stiffness and the smallest displacement under a torque of 5 N·m, indicating its effectiveness in preventing rotational displacement at the fracture site following fixation. Although the torsional stiffness of the NEF was slightly lower than that of UEF, it remained at a high level, effectively reducing shear forces and promoting fracture healing. In contrast, the externalized locking compression plate (E-LCP) displayed the lowest torsional stiffness, resulting in significant rotational displacement under the same applied torque, which is detrimental to callus formation and overall fracture healing.

Following the methodology of Kanchanomai et al. [13], we conducted 108,000 cycles of axial compression fatigue testing, simulating six months of postoperative activity in adults (assuming 600 daily steps). None of the four groups experienced device failure during the fatigue tests, suggesting that the NEF and other methods can withstand prolonged physiological loading without mechanical compromise. This endurance ensures structural integrity during early healing phases, where repetitive loading from partial weight-bearing or rehabilitation exercises is common. The ultimate compressive load of E-LCP was the smallest (1564.900 N), suggesting that all four fixation methods can all withstand the weight load of an average adult. Notably, the NEF's **ultimate load capacity (5307 N)** far exceeds the average axial load during single-leg stance (700 N), providing a safety margin for patients with higher body weights or dynamic activities. Previous studies have reported that the failure rate of internal fixation plates in fracture treatment is approximately 7% [30]. In the context of osteoporotic fractures, refracture at the lower end of the plate is a common complication of traditional plate fixation, with an incidence of 1–3% [31]. In this experiment, all fractures occurred at the lowest screw of the fixation device under extreme axial compression loads, which may be attributed to the weaker anatomical structure of the transition between the middle and lower tibia or the stress shielding effect of the fixation device.

While the NEF demonstrates superior biomechanical performance, potential clinical risks warrant discussion. Similar to traditional external fixation systems, pin tract infections remain a concern due to percutaneous screw placement; however, the NEF's full threaded screws may increase tightness with soft tissue, potentially lowering infection risks compared to conventional external fixators (UEF). Additionally, the bicortical locking screws, while enhancing stability, carry a theoretical risk of neurovascular injury during insertion, necessitating precise surgical technique. Compared to traditional external fixators (UEF) and externalized locking compression plates (E-LCP), the NEF's deepened thread-locking mechanism mitigates screw-frame loosening during prolonged lower-limb rehabilitation, thereby reducing the risk of fixation failure. This enhanced angular stability ensures sustained construct integrity under cyclic loading, a critical advantage for patients requiring extended immobilization or early weight-bearing protocols. Future iterations may incorporate antimicrobial coatings or modular dynamization to further optimize safety.

The NEF exhibited superior biomechanical performance over conventional methods, with a compact design enabling minimally invasive application while maintaining structural integrity. This reduces soft tissue trauma and postoperative morbidity. In a preliminary clinical trial, a 62-year-old male with an open tibiofibular fracture (Gustilo type IIIA) secondary to chainsaw injury underwent NEF fixation. The frame was positioned over the anteromedial tibia, secured by four bicortical locking screws on both fracture sides under fluoroscopic guidance. Negative-pressure wound therapy (VSD) was applied postoperatively for 3–5 days. Radiographic follow-ups at 4-week intervals confirmed progressive fracture consolidation without evidence of pin tract infection, screw loosening, or hardware failure. Complete union was achieved at 12 weeks, permitting device removal. Full knee and ankle range of motion was restored post-rehabilitation. The study received ethics approval from Chinese PLA General Hospital (No. S2021-345-01) with informed consent obtained. These outcomes position NEF as a promising alternative for tibial fracture management, warranting further multicenter validation.

The novel external fixator (NEF) offers distinct clinical advantages over traditional methods. Its controlled micromotion (0.512 mm displacement under 700 N) aligns with the mechanobiological principles of fracture healing, promoting callus formation by stimulating osteoblast activity and angiogenesis at the fracture site [9, 32]. Compared to rigid internal fixation (LCP), which suppresses callus development due to excessive stiffness, the NEF's intermediate stiffness balances mechanical stability and biological stimulation, potentially accelerating union in comminuted fractures. Clinically, the compact design minimizes soft tissue irritation, enabling earlier mobilization and reducing postoperative pain, as evidenced by our preliminary trial where a patient regained full knee/ankle mobility within 12 weeks. Additionally, the raised screw holes and 20 mm plate-skin distance mitigate skin necrosis risks, addressing a common complication of conventional external fixators. While direct clinical data on osteogenesis rates are pending, biomechanical parallels to dynamized plating systems [10] suggest comparable or superior healing outcomes, warranting further prospective studies.

This study has several limitations. First, in the finite element analysis (FEA) the bone geometry was simplified to a hollow cylindrical structure, omitting anatomical features such as cortical-cancellous bone differentiation, medullary cavity variations, and surface irregularities. This simplification may have altered stress distribution patterns compared to real-world scenarios. Second, the experimental design does not fully simulate the postoperative activities of patients, particularly the rotational loads and angular stresses that occur during weight-bearing exercises. Additionally, the effects of osteoporosis, fracture type, muscle, and other soft tissues on the mechanical behavior were not considered. To address these limitations, future studies could employ patient-specific bone geometries derived from CT/MRI scans [33], integrate viscoelastic soft tissue models, and incorporate dynamic loading protocols to better simulate in vivo conditions. Additionally, validation through cadaveric experiments or in silico multibody simulations could enhance the clinical relevance of FEA and biomechanical test predictions.

Conclusion

Both finite element analysis and mechanical testing demonstrated that the novel external fixation device exhibited excellent compressive stiffness and torsional strength. Furthermore, the device successfully withstood over 100,000 cycles of fatigue testing, validating the rationality of its design and confirming its feasibility for use in the treatment of tibial fractures.

Supplementary Information

The online version contains supplementary material available at https://doi.org/10.1186/s13018-025-05681-8.

Supplementary Material 1

Supplementary Material 2

Acknowledgements
Not applicable.

Author contributions
S.L was involved in study design, data collection, report writing, and manuscript review. S.Y.L and Z.G participated in study design, data collection, and analysis. W.X was responsible for experimental analysis and manuscript review. X.L and Y.L contributed to study design, report writing, and manuscript review. All authors reviewed and approved the manuscript.

Funding
This work was supported by the grants from the Sponsored by Science Foundation of AMHT (2022YK23) and from the China Healthy Longevity Catalyst Awards (2023-JKCS-26).

Data availability
No datasets were generated or analysed during the current study.

Declarations

Ethics approval and consent to participate
Not applicable.

Consent for publication
Not applicable.

Competing interests
The authors declare no competing interests.

Received: 15 January 2025 / Accepted: 4 March 2025
Published online: 28 March 2025

References

1. Zhou Y, Zhu Y, Zhang X, Tian D, Zhang B. Comparison of radiographic and functional results of die-punch fracture of distal radius between volar locking plating (VLP) and external fixation (EF). J Orthop Surg Res. 2019;14(1):373.
2. Shannon FJ, Mullett H, O'Rourke K. Unreamed intramedullary nail versus external fixation in grade III open tibial fractures. J Trauma. 2002;52(4):650–4.
3. Marti R, Besselaar PP. [Use of the AO plate as external fixation]. Ztschrift Fur Orthopadie Und Ihre Grenzgebiete. 1984;122(2):225.
4. Ma CH, Tu YK, Yeh JH, Yang SC, Wu CH. Using external and internal locking plates in a two-stage protocol for treatment of segmental tibial fractures. J Trauma Acute Care Surg. 2011;71(3):614–19.
5. Liu W, Yang L, Kong X, An L, Hong G, Guo Z et al. Stiffness of the locking compression plate as an external fixator for treating distal tibial fractures: a biomechanics study. BMC Musculoskelet Disord 2017;18.
6. Zhou SQ, Zhang Q, Ding XD, Qin YY, Cai S. [Locking plate external fixation combined with membrane induction technology for the treatment of open and comminuted tibial fractures with bone defects]. Zhongguo Gu Shang. 2021;34(5):400–5.
7. Ahmad M, Nanda R, Bajwa AS, Candal-Couto J, Green S, Hui AC. Biomechanical testing of the locking compression plate: when does the distance between bone and implant significantly reduce construct stability? Injury-international J Care Injured. 2007;38(3):358–64.
8. Kenwright J, Goodship A. Controlled mechanical stimulation in the treatment of tibial fractures. Clin Orthop Relat Res 1989:36–47.
9. Bottlang M, Doornink J, Lujan T, Fitzpatrick D, Marsh J, Augat P, et al. Effects of construct stiffness on healing of fractures stabilized with locking plates. J Bone Joint Surg Am Volume. 2010;92(Suppl 2):12–22.
10. Bottlang M, Shetty SS, Blankenau C, Wilk J, Tsai S, Fitzpatrick DC et al. Advances in dynamization of plate fixation to promote natural bone healing. J Clin Med 2024;13(10).
11. Augat P, Penzkofer R, Nolte A, Maier M, Panzer S, v Oldenburg G, et al. Interfragmentary movement in diaphyseal tibia fractures fixed with locked intramedullary nails. J Orthop Trauma. 2008;22(1):30–6.
12. Barcik J, Epari DR. Can optimizing the mechanical environment deliver a clinically significant reduction in fracture healing. Time? Biomedicines 2021;9(6).
13. Kanchanomai C, Phiphobmongkol V. Biomechanical evaluation of fractured tibia externally fixed with an LCP. J Appl Biomech. 2012;28(5):587–92.
14. Kowalski MJ, Schemitsch EH, Harrington RM, Chapman JR, Swiontkowski MF. A comparative Biomechanical evaluation of a noncontacting plate and currently used devices for tibial fixation. J Trauma Acute Care Surg. 1996;40(1):5–9.
15. Ang BFH, Chen JY, Yew AKS, Chua SK, Chou SM, Chia SL, et al. Externalised locking compression plate as an alternative to the unilateral external fixator: a Biomechanical comparative study of axial and torsional stiffness. Bone Joint Res. 2017;6(4):216–23.
16. Azevedo Filho FASD, Cotias RB, Azi ML, Teixeira AADA. Reliability of the radiographic union scale in tibial fractures (RUST). Revista Brasileira De Ortop. 2017;52(1):35–9.
17. Yu Z, Yanbiao W, Lifeng L et al. Locking compression plate as an external fixator in the treatment of closed distal tibial fractures. Int Orthop 2015.
18. Hidayat L, Triangga AFR, Cein CR, Irfantian A, Rahayu BFP, Resubun AP, et al. Low profile external fixation using locking compression plate as treatment option for management of soft tissue problem in open tibia fracture grade IIIA: A case series. Int J Surg Case Rep. 2022;93:106882.
19. Ma CH, Wu CH, Yu SW, Yen CY, Tu YK. Staged external and internal less-invasive stabilisation system plating for open proximal tibial fractures. Injury-international J Care Injured. 2010;41(2):190–96.
20. Luo P, Xu D, Wu J, Chen YH. Locked plating as an external fixator in treating tibial fractures: A PRISMA-compliant systematic review. Med (Baltim). 2017;96(49):e9083.
21. Li W, Chen Y, Zhuang Q. Management of complex open tibial plateau fracture: A case report on the application of locked plate external fixation technique during bone callus formation stage to replace transarticular external fixation. Orthop Rev (Pavia). 2024;16:94035.
22. Mubarak FS, Kanagaratnam K. Placing locking compression plates as an external fixator in wild animal (Crocodile) bite victim: A case report. Cureus. 2023;15(10):e47511.
23. Ma CH, Chiu YC, Tsai KL, Tu YK, Yen CY, Wu CH. Masquelet technique with external locking plate for recalcitrant distal tibial nonunion. Injury. 2017;48(12):2847–52.
24. Bangura ML, Luo H, Zeng T, Wang M, Lin S, Chunli L. Comparative analysis of external locking plate and combined frame external fixator for open distal tibial fractures: a comprehensive assessment of clinical outcomes and financial implications. BMC Musculoskelet Disord. 2023;24(1):962.
25. Blažević D, Kodvanj J, Adamović P, Vidović D, Trobonjača Z, Sabalić S. Comparison between external locking plate fixation and conventional external fixation for extraarticular proximal tibial fractures: a finite element analysis. J Orthop Surg Res. 2022;17(1):16.
26. Su H, Zhong S, Ma T, Wu W, Lu Y, Wang D. Biomechanical study of the stiffness of the femoral locking compression plate of an external fixator for lower tibial fractures. BMC Musculoskelet Disord. 2023;24(1):39.
27. Güvercin Y, Abdioğlu AA, Dizdar A, Yaylacı EU, Yaylacı M. Suture button fixation method used in the treatment of syndesmosis injury: A Biomechanical analysis of the effect of the placement of the button on the distal tibiofibular joint in the mid-stance phase with finite elements method. Injury. 2022;53(7):2437–45.
28. Güvercin Y, Yaylacı M, Dizdar A, Kanat A, Uzun Yaylacı E, Ay S, et al. Biomechanical analysis of odontoid and transverse Atlantal ligament in humans with ponticulus posticus variation under different loading conditions: finite element study. Injury. 2022;53(12):3879–86.
29. External fixation using. Locking plate in distal tibial fracture: a finite element analysis. Eur J Orthop Surg Traumatol. 2015;25(6):1099–104.
30. Riemer BL, Butterfield SL, Burke CJ, Mathews D. Immediate plate fixation of highly comminuted femoral diaphyseal fractures in blunt polytrauma patients. Orthopedics. 1992;15(8):907.
31. Beaupré GS, Giori NJ, Caler WE, Csongradi J. A comparison of unicortical and bicortical end screw attachment of fracture fixation plates. J Orthop Trauma. 1992;6(3):294–300.
32. Claes L. Biomechanical principles and mechanobiologic aspects of flexible and locked plating. J Orthop Trauma. 2011;25(Suppl 1):S4–7.
33. Güvercin Y, Yaylacı M, Dizdar A, Özdemir ME, Ay S, Yaylacı EU, et al. Biomechanical analysis and solution suggestions of screw replacement scenarios in femoral neck fracture surgeries: finite element method. Orthop Surg. 2025;17(2):614–23.

Publisher's note